

# Difference in signals from a mid-ocean shot at hydrophones near Diego Garcia and Cape Leeuwin

**Marshall V. Hall**

Emeritus Scientist, DSTO Sydney, Pyrmont NSW, Australia

## ABSTRACT

Oceanic sound velocity profiles can vary so as to change important characteristics of transients propagated over long distances. Staff of the Scripps Institution of Oceanography fired a series of deep shots during a transit across the Indian Ocean in 2003. The shot to be considered was a Signal Underwater Sound (SUS), fired on 29 May at a depth of 0.9 km in the middle of the ocean. The acoustic signals were recorded with hydrophones south of Diego Garcia (DGS), and off Cape Leeuwin (CL). These hydrophones were respectively 1600 km and 4260 km from the shot. It was noted that the DGS signal had its peak near the start, whereas the peak of the CL signal was at the end. For a frequency of 100 Hz, the mode travel times and attenuations along each path have been computed, using sound velocity profiles based on average temperature and salinity profiles. Since the source and receivers were near the SOFAR axis, the transmission losses of the modes generally increase as the mode number increases. Along the path to DGS, the sound velocity profile is relatively blunt. As a result, the low-order modes travel faster than the contributing (non-attenuated) modes of somewhat higher order. Along the path to CL the sound velocity profile is relatively sharp and Mode 1 is slow, regardless of seafloor depth. The difference between the signals can thus be attributed to the different sound velocity profiles along the respective paths.

## INTRODUCTION

It has been known since the 1940s that low frequency sound (below 1 kHz) can travel very long distances in the deep ocean. This is due to the temperature and pressure acting on the sound velocity in such a way as to produce a minimum in the sound velocity profile (SVP), which provides a long-range acoustic SOFAR channel. The axis depth varies with latitude, but is generally about 1 kilometre below the surface.

In the past, the common scenario has been a shallow source and receiver. In this case the phenomenon of the convergence zone occurs, providing the seafloor depth (SFD) is sufficiently great. For most scenarios, these zones are spaced 60 km apart and are initially around 8 km wide (their width increases gradually from one to the next). The peak Sound Pressure Level (SPL) is around 20 dB higher than the corresponding value in a homogeneous medium (Hale, 1961). There is interaction with the sea surface in each zone, although the consequent scattering is unimportant at low frequencies. In order to avoid loss of energy due to interaction with the seabed, the SFD must be such that the sound velocity at that depth exceeds its value at the surface. In temperate latitudes a SFD of 3 km may be sufficient, whereas in tropical latitudes a SFD of 5 km will be necessary.

This paper will however be concerned with a source and receiver near the SOFAR axis. In this scenario there are travelling soundwaves that remain at depths near the axis and do not interact with either the sea surface or the seabed, unless a seafloor feature protrudes into the channel. Without such interaction, the only loss of energy is cylindrical spreading and a very small absorption due to the properties of seawater.

Explosions are powerful sources of broadband sound. Shots from small (0.8 kg) charges of TNT have been readily detected over oceanic propagation paths, using the low frequency sound they produce. Shot location is done by triangulation using travel times to a number of hydrophones. Care is needed in selecting the appropriate arrival time. In

some regions, such as the deep North Atlantic, the signal from a shot on the SOFAR axis "is characterized by multiple arrivals that increase in tempo and amplitude until there is a sharp cutoff" (Hirsch, 1965). SOFAR shots were recorded with a seafloor hydrophone off New Zealand at a depth of 1.1 km. The onset was abrupt and there was a gradual decay in level (Guthrie, 1974). The travel time is therefore determined by the end of the signal in some cases, and by the start in others.

A study was made in 1960 of the localisation accuracy to be expected from SOFAR shots to a seafloor hydrophone in the SOFAR channel, at ranges up to 8700 km (Bryan et al, 1963). The following conclusions were drawn:

- It should be possible to obtain an accuracy of 50 m at a range of 2000 km from a sample of 20 shots
- Off-axis shooting seriously affects the accuracy
- Large topographic features which do not intersect the SOFAR axis sever the start of the signal without impairing arrival time accuracy (the peaks occurred near the end)

The SPL for source and receiver on the SOFAR axis does exhibit the features of convergence, although not to the same degree as for shallow source and receiver. The mechanism is different, and the asymmetry of the SVP around the SOFAR axis reduces the focussing effect to a difference of 2 to 3 dB. For a simplified North Atlantic scenario, the theoretical distance between focussing ranges has been found to be 26 km (Williams and Horne, 1967).

During May and June 2003, staff of the Scripps Institution of Oceanography conducted experiments in which a series of 0.85-kg Signal Underwater Sound (SUS) shots were fired while transiting the Indian Ocean (Blackman et al, 2003). The shot to be considered here was fired on 29 May at a depth of 915 m at station A6 in the middle of the ocean (-22.1°, 72.7°). At this depth, the bubble-pulse period of that SUS is

6.7 milliseconds, giving a spectral peak at 150 Hz. Estimates of the Source Level spectrum are shown in Figure 1. One estimate was obtained by “scaling” from Source Level data for a firing depth of 99 m (Chapman, 1988), and the other from a theoretical spectrum (Zhang, 1998) based on waveform parameters measured with firing depths between 30 and 200 m (Chapman 1985). At frequencies below 150 Hz, the spectrum of the emitted signal has a slope of approximately 10 dB per octave.

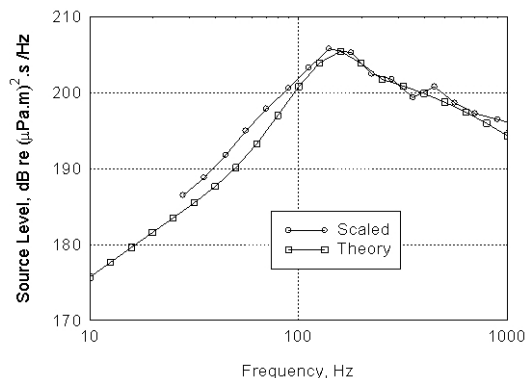


**Figure 1.** Estimated Source Level spectrum of a 0.85-kg SUS charge fired 915 m deep.

The acoustic signals were recorded at two hydrophone stations installed by the Comprehensive Test Ban Treaty Organisation (CTBTO). One station is south of Diego Garcia (DGS) at  $(-7.6^\circ, 72.5^\circ)$  and the other is south-west of Cape Leeuwin (CL) at  $(-34.9^\circ, 114.2^\circ)$ . Each of these stations contains a triplet of hydrophones, spaced horizontally around 2 km apart. The hydrophones produce data over the band from 2 Hz to 120 Hz. The geoid distances from the shot to the stations are 1598 km and 4261 km respectively. It was noted that the DGS signal had its peak near the start, whereas the peak of the CL signal was at the end. The objective of this paper is to explain this difference

## METHOD

### Acoustic modelling

The algorithms available for calculating TL are of the following four types:

- Direct integration of the Bessel transform of the Greens function
- Normal modes
- Parabolic Equation
- Rays

For the present analysis, a normal-mode algorithm is the most practicable, since the required information on signal TL as a function of time may be estimated from the properties of the individual modes. Of the normal-mode algorithms available, ORCA (Westwood et al, 1996) has been the one used. ORCA requires that the environment that constitutes the acoustic waveguide be range-independent. For a particular run, only one SVP and geo-acoustic model of the seabed can be supplied. ORCA assumes that the waveguide boundaries are horizontal straight lines.

For ranges comparable with the earth radius ( $R_E$ ) of 6370 km, the ocean is more correctly modelled as a spherical shell than as a flat layer, since rays diverge horizontally less than they would in a flat waveguide (and they reconverge as they approach the antipode of their source). The cylindrical

spreading loss of  $10 \log(r)$  should be replaced by  $10 \log [R_E \sin(r/R_E)]$  (McDonald et al, 1994). ORCA does not allow for this effect, but the difference is only 0.3 dB at a range of 4260 km. Another consequence of the earth's (quasi) sphericity is that vertical lines converge with increasing depth. This can be taken into account by adding small “earth flattening” corrections to the depth and sound velocity (Watson, 1958).

### Reference Sound Velocity Profile

In a study of dispersion in SOFAR propagation, Pedersen and White (1970) presented a detailed analysis and numerical investigation of the ray theory of four simple SVPs in common use as models of the deep sound channel. They determined the near-axial ray-theory properties of a SVP, and concluded that a cosh SVP represents the transition between the two types of SVP for which the axial ray is slower or faster than near-axial rays. In a recent study of normal modes, it has been found that mode group velocities are independent of mode number for a cosh SVP. Details are given in the Appendix. A similar study for a bi-cosh profile (made by joining two cosh functions) is in progress.

### The Environment

In order to compute acoustic travel times and transmission loss (TL) along each path, SVPs were calculated with Mackenzie's (1981) expression, using temperature and salinity profiles from the World Ocean Atlas (1998) at representative positions. In this atlas, either a 1-degree or a 5-degree averaging square may be selected, and for this process the latter was chosen (the former were more liable to have profiles of limited depth coverage). Six positions were selected for study, as listed in Table 1. This atlas has separate results for the four quarters of the year, and since the acoustic experiment occurred in May, the second quarter (Autumn in the southern hemisphere) was selected

**Table 1.** The six SVPs studied

SVP #	Latitude	Longitude
1	$-10^\circ$	$75^\circ$
2	$-15^\circ$	$70^\circ$
3	$-20^\circ$	$75^\circ$
4	$-30^\circ$	$95^\circ$
5	$-35^\circ$	$110^\circ$
6	$-35^\circ$	$115^\circ$

In the few cases where the data available did not extend to the seafloor, they were extrapolated using deep data from nearby regions. Of the six SVPs, # 1 is similar in shape to that of a bi-cosh curve. A single cosh curve cannot be used, due to the asymmetry of the SVP about the SOFAR axis. Profiles 1 and 3, together with a suitable bi-cosh function, are shown in Figure 2. The other profiles have shapes that are sharper than a bi-cosh curve, in that the SVP minimum is less than the minimum of a bi-cosh curve that otherwise would be a good fit to the SVP. Profiles 4 and 6 are shown in Figure 3. The amount by which the bi-cosh minimum exceeds the actual SVP minimum increases as the latitude approaches  $-35^\circ$ .

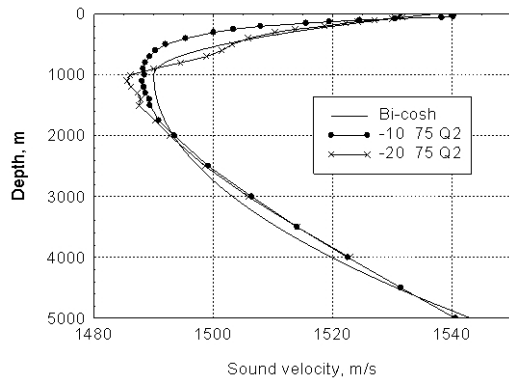


**Figure 2.** A bi-cosh profile and average Sound velocity profiles for Autumn at positions in the central tropical Indian Ocean. The legend shows the latitude, longitude, and season (quarter).

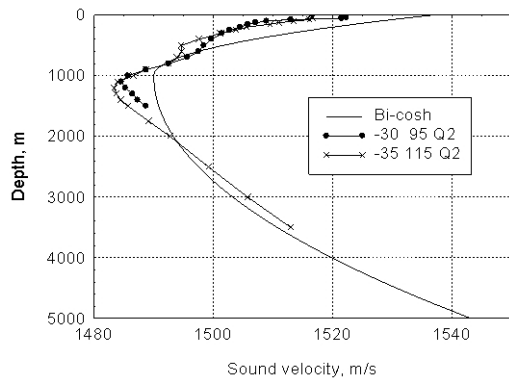


**Figure 3.** The bi-cosh profile and average Sound velocity profiles for Autumn at positions in the eastern temperate Indian Ocean.

The linear topographies of the seafloor along the geoid paths between the source and the two receivers were obtained using the ETOPO2 database (National Geophysical Data Center, n.d.). The results are shown in Figure 4 as a function of range from A6. To improve clarity, range toward CL has been made negative.

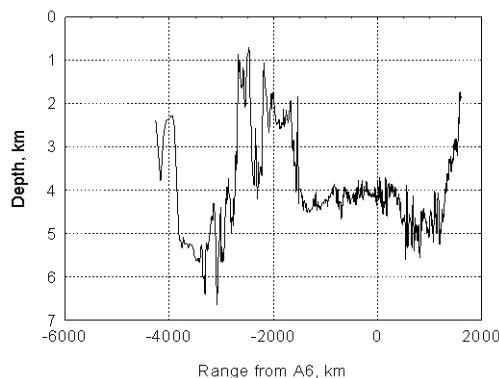


**Figure 4.** Seafloor depth as a function of range from Scripps Institute of Oceanography station A6 in the central tropical Indian Ocean. Positive range describes the path to DGS; negative range describes the path to CL.

**Calculations of the acoustic signal**

In view of the large variations in SFD along the paths, a rigorous approach would entail using a TL algorithm that could be supplied a range-dependent environment. The present analysis attempts to draw useful conclusions by judicious use of range-independent calculations, combined with theoretical reasoning.

A frequency of 100 Hz was selected for the calculations, since the measured signal-to-noise ratio increased monotonically with frequency until the upper limit of 125 Hz was approached.

ORCA runs were conducted for SVPs # 1 and 4, with SFDs of both 2 and 5 km (a total of four runs). Runs were not conducted for profiles # 2, 3, 5 and 6, since it was adjudged that their properties could be estimated by interpolating between the properties found for # 1 and 4. The earth flattening corrections have not been applied, and will be commented on where appropriate.

The geo-acoustic model was held fixed, with a sound velocity of 1540 m/s, a density of 1.5, and an absorption coefficient of 1 dB per wavelength (the shear velocity was assumed to be zero).

ORCA produces results for damping (rate of attenuation with range), group velocity and complex pressure of the individual modes. The number of modes required for an accurate calculation depends on the minimum range of interest since the shorter this range, the greater the number of modes that need to be computed (mode damping generally increases with mode number). In order to keep the number of modes to a value appropriate to this analysis, ORCA was instructed to cease the search for further modes once the damping rate reached 0.1 dB /km, although a smaller threshold could have been used (over a distance of 1600 km, the threshold mode would attenuate by 160 dB).

In order to generate a simulation of the intensity of the signal as a function of time, the travel times of the modes were calculated from their group velocities. For a pulse of a given duration, modes that overlap will give rise to an increase in signal intensity (unless they are out of phase), while modes that do not overlap will cause dispersion of the signal. For shots, the effective pulse duration is the reciprocal of the filter bandwidth, and for the present analysis this duration has been assumed to be 0.2 seconds. Guthrie (1974) used a duration of 0.1 seconds for his deep ocean study, but this value yielded a large number of vacant time intervals when tried in the present analysis.

The intensity of each time interval was then computed by summing the complex pressures of the modes that arrive during the interval. Coherent mode summation is the appropriate procedure if the relative phases of the modes are known. The alternative of incoherent summation would be appropriate if the relative phases are randomly spaced over a whole cycle. Although the relative phases are unlikely to be accurately known after travelling thousands of kilometres, it is also unlikely that they are spread over a whole cycle. To determine the significance of this aspect, the intensities were re-calculated using incoherent summation. The greatest differences are less than 10 dB, occur where there are many modes contributing, and make no difference to the objective of this study.

**RESULTS**

**Sound Velocity Profile # 1**

With this SVP, the number of modes computed for the two SFDs are 32 and 140 respectively. The Mode group velocities are shown in Figure 5. The earth flattening correction increases the group velocities by 0.3 m/s. For the 5-km SFD, group velocity initially declines, passes through a minimum and gradually increases to a maximum at Mode 126. For the 2-km SFD, group velocity monotonically declines, and separates from the 5-km curve at Mode 11.

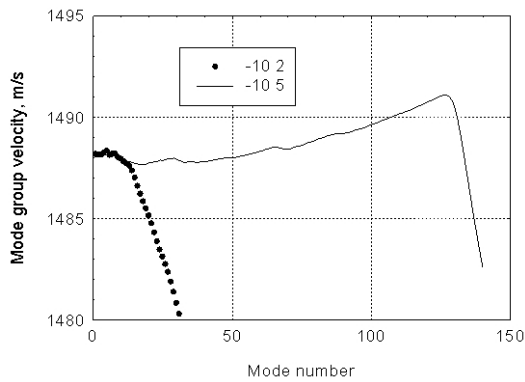


**Figure 5.** Mode group velocities at frequency 100 Hz for the sound velocity profile at position # 1. The numerals in the legend denote latitude ( $-10^\circ$ ) and SFDs of 2 and 5 km.

The TLs of individual modes from A6 to DGS have been computed using SVP # 1. The results are shown in Figure 6. Since the source and receivers are near the SOFAR axis, the mode TLs generally increase as the mode number increases. The mode-to-mode fluctuation is due to the fact that the source and receiver depths will sometimes be near zeroes of the depth functions of particular modes. The earth flattening correction does not alter the average TLs of the individual modes, but does change the mode number at which a characteristic of the curve (such as a peak) occurs. This change increases with mode number, and there is no change for the first 10 modes.

The minimum TL (maximum intensity) occurs at mode 5 for both SFDs. It can be seen that the propagation velocity and TL of the peak will remain constant as SFD varies between 2 and 5 km.

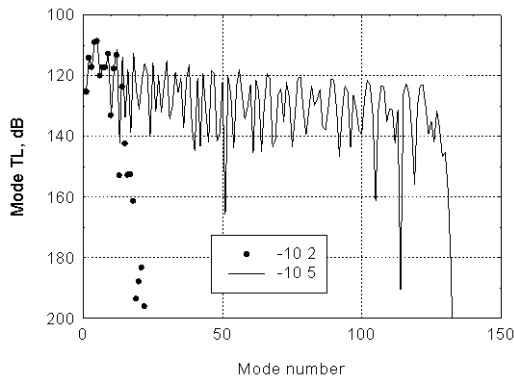


**Figure 6.** Transmission Losses of individual modes, at frequency 100 Hz from A6 to DGS, using the sound velocity profile at position # 1. The numerals in the legend denote latitude ( $-10^\circ$ ) and SFDs of 2 and 5 km.

The numbers of modes that arrive in successive time intervals (with a fixed aperture of 0.2 seconds) have been computed, and the results are shown in Figure 7. The first interval begins at 1071.7 s, the arrival of the fastest mode. Applying the earth flattening correction would decrease that by 0.2 s. For the 5-km SFD, several modes arrive in the early intervals, and there is a sharp peak in the number of modes at a travel time of 1073.9 s (due to the slow variation of group velocity with mode number for this SFD). For the 2-km SFD, there is no arrival until 1073.7 s, and eight arrive in the first interval.

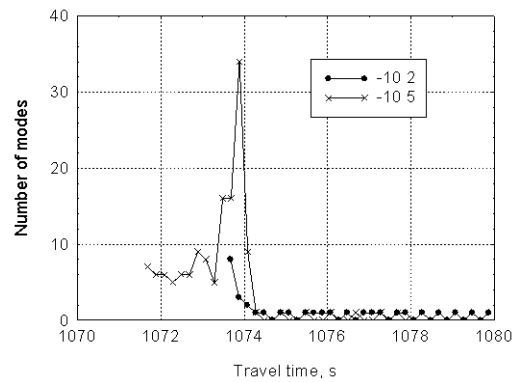


**Figure 7.** Temporal variation of the number of modes arriving at DGS from A6, in each time interval of 0.2 s. The numerals in the legend denote latitude ( $-10^\circ$ ) and SFDs of 2 and 5 km.

The simulated signals, expressed as TL as a function of time, are shown in Figure 8. The 5-km SFD signal begins at low level at 1071.7 s, fluctuates for 2 s, rises to a peak at 1073.9 s, and then stops abruptly (the earth flattening correction would decrease these time by 0.2 s). The 2-km signal begins at 1073.7 s and immediately commences an almost monotonic decay. It can be seen in Blackman et al (2003) that the signals measured with DGS hydrophones 1 and 2 had peaks at 1073 s that began abruptly and decayed over 2 or 3 seconds. The peak for hydrophone 3 arrived 2 seconds later; this hydrophone is north of the other two.

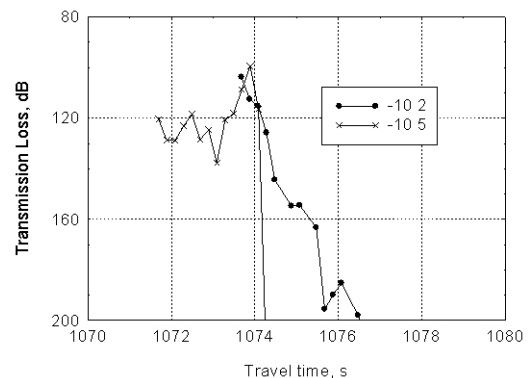


**Figure 8.** Temporal variation of the Transmission Loss from A6 to DGS, in each time interval of 0.2 s. The numerals in the legend denote latitude ( $-10^\circ$ ) and SFDs of 2 and 5 km.

#### Sound Velocity Profile # 4

With this SVP, the number of modes computed for the two SFDs are 38 and 137. The variations of group velocity with mode are shown in Figure 9 (again, the earth flattening correction would increase these by 0.3 m/s). For the 5-km SFD, group velocity increases almost monotonically to a maximum at mode 84 and gradually increases to another maximum at Mode 125. For the 2-km SFD, group velocity increases to a maximum at mode 13, where it has separated from the 5-km curve.

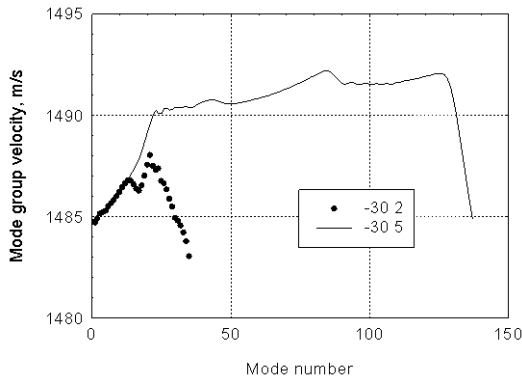


**Figure 9.** Mode group velocities at frequency 100 Hz for the sound velocity profile at position # 4. The numerals in the legend denote latitude (-30°) and SFDs of 2 and 5 km.

The results for TL of the individual modes from A6 to CL are shown in Figure 10. The minimum TL occurs at mode 6 for both SFDs. The propagation velocity and TL of the peak again remain constant as SFD varies between 2 and 5 km.

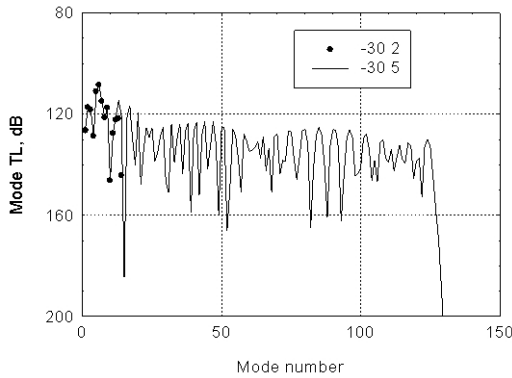


**Figure 10.** Transmission Losses of individual modes at frequency 100 Hz from A6 to CL using the sound velocity profile at position # 4. The numerals in the legend denote latitude (-30°) and SFDs of 2 and 5 km.

The numbers of modes that arrive in the successive 0.2-s time intervals are shown in Figure 11. The first interval begins at 2855.5 s, the arrival of the fastest mode. For the 5-km SFD, several modes arrive in the early intervals, and there is a sharp peak in the number of modes at a travel time of 2856.7 s (due to the slow variation of group velocity between modes 90 and 110 for this SFD). There are two further peaks at 2858.5 s and 2858.9 s, due to slow variation in group velocity in the neighbourhood of mode 50. For the 2-km SFD, there is no arrival until 2863.5 s. The earth flattening correction would decrease these times by 0.6 s.

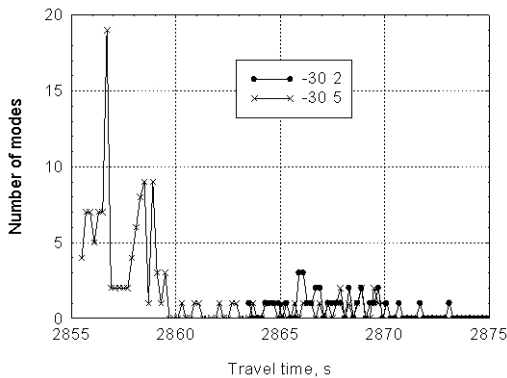


**Figure 11.** Temporal variation of the number of modes arriving at CL from A6, in each time interval of 0.2 s. The numerals in the legend denote latitude (-30°) and SFDs of 2 and 5 km.

The simulated signals are shown in Figure 12. The 5-km SFD signal begins at low level at 2855.5 s, fluctuates for 10 s, rises to a peak at 2868.3 s, and then stops abruptly. The 2-km SFD signal begins at 2865.9 s, fluctuates, rises to a peak at 2868.3 s, and stops abruptly at 2869.7 s. Again, the earth flattening correction would decrease these times by 0.6 s. The signals measured with CL hydrophones 2 and 3 rose for one or two seconds to a peak at 2869 s and then stopped abruptly. The peak for hydrophone 1 arrived one second later; this hydrophone is east of the other two

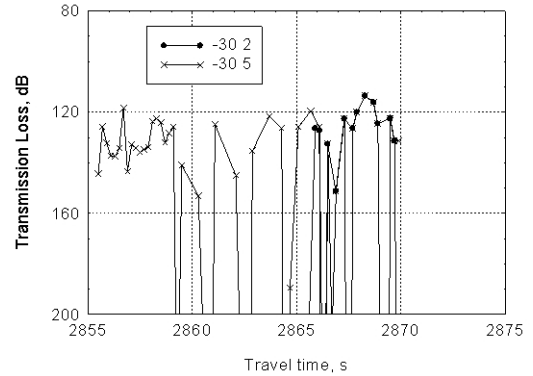


**Figure 12.** Temporal variation of the Transmission Loss from A6 to CL, in each time interval of 0.2 s. The numerals in the legend denote latitude (-30°) and SFDs of 2 and 5 km.

**CONCLUSIONS**

A bi-cosh (or cosh) SVP is non-dispersive since it yields mode group velocities independent of mode number. For a SVP blunter than a bi-cosh curve the group velocities decrease with mode number, and the signal peak occurs at the beginning. For a sharper SVP the group velocities increase with mode number, and the signal peak occurs at the end.

Near Diego Garcia, the SOFAR channel is sometimes slightly blunter than a cosh curve.

Near Cape Leeuwin, the SOFAR channel is always sharper than a cosh curve.

For SFD between 2 and 5 km, the travel time and TL of the signal peak are independent of SFD.

If the SFD is large (c. 5 km), the peak of the SOFAR signal occurs at the end of the observable signal, for all the Indian Ocean SVPs studied

According to mode theory, the effects of reducing SFD (to c. 2 km) are:

- The observed signal is shortened. For a SOFAR channel blunter than a cosh curve, the signal peak occurs at the start.
- For a SOFAR channel sharper than a cosh curve, the signal peak occurs at the end.

**APPENDIX: MODAL GROUP VELOCITIES FOR A COSH SOUND VELOCITY PROFILE.**

For any SVP described by a function  $C(z)$ , the Helmholtz equation for the depth-dependent factor  $Z(z)$  in the expression for sound pressure is (Brekhovskikh, 1980, page 323):

$$Z(z)'' + \gamma(z)^2 Z(z) = 0.$$

where  $\gamma(z)$  is the vertical wavenumber, given by  $\gamma^2(z) = \omega^2/C(z)^2 - \xi^2$ , in which  $\xi$  is the horizontal wavenumber.  $\xi$  takes on a sequence of eigenvalues, as determined by constraints on  $Z(z)$ . In depth intervals where  $\gamma(z)^2 > 0$ ,  $Z$  is an oscillatory function of  $z$ , otherwise  $Z$  is an evanescent function of  $z$ . A medium will act as a waveguide at a given frequency only if it contains at least one depth interval over which  $\gamma(z)^2 > 0$ .

The cosh SVP with the axis at  $z = 0$  is given by  $C(z) = C_0 \cosh(z/H)$ . For this  $C(z)$ , the solution to the Helmholtz equation is (Brekhovskikh, 1980, page 424):

$$Z(z) = m! P[j, m, \tanh(z/H)],$$

where  $P$  is the associated Legendre function of degree  $j$  and order  $m$ ,  $m = \xi H$ , and  $j$  is given by  $j(j+1) = (\omega H/C_0)^2$ . Since this last parameter is generally large,  $j \approx \omega H/C_0$ .

The associated Legendre function  $P[j, m, x]$  is proportional to the  $m$ 'th derivative of the Legendre polynomial of degree  $j$  with respect to  $x$ , and thus  $P[j, m, x] = 0$  for  $m > j$  (Korn & Korn 1961, page 736). Since there is no other constraint on  $Z(z)$ , the values of  $m$  are the integers up to  $j - 1$  (if  $m = j$  the vertical wavenumber is not positive at any depth). The characteristic equation that determines the eigenvalues  $\xi_n$  is therefore

$$\xi_n H = \omega H/C_0 - n, \quad n = 1, 2, \dots$$

The group velocity  $V$  of mode  $n$  is given by (Brekhovskikh, 1980, page 341)

$$V_n = (d\xi_n/d\omega)^{-1}.$$

For the cosh SVP, the group velocities are therefore given by

$$V_n = C_0 \text{ (a constant).}$$

## REFERENCES

- Blackman, D. K., Mercer, J. A., Andrew, R., de Groot-Hedlin, C., & Harben, P. 2003, "Indian Ocean Calibration Tests: Cape Town-Cocos Keeling 2003", *Proceedings of the 25th Seismic Research Review*, pp. 517-523. Retrieved: June 2005, from <https://www.nemre.nnsa.doe.gov/cgi-bin/prod/researchreview/index.cgi?Year=2003>
- Brekhovskikh, L. M. 1980, "Waves in Layered Media", (English translation), Second Edition, Academic Press, New York.
- Bryan, G. M., Truchan, M., & Ewing, J. I. 1963, "Long-range SOFAR studies in the South Atlantic Ocean", *Journal of the Acoustical Society of America*, vol. 35, pp. 273 - 278.
- Chapman, N. R. 1985, "Measurement of the waveform parameters of shallow explosive charges", *Journal of the Acoustical Society of America*, vol. 78, pp. 672 - 681.
- Chapman, N. R. 1988, "Source levels of shallow explosive charges", *Journal of the Acoustical Society of America*, vol. 84, pp. 697 - 702.
- Guthrie, K. M. 1974, "Wave theory of SOFAR signal shape", *Journal of the Acoustical Society of America*, vol. 56, pp. 827 - 836.
- Hale, F. E. 1961, "Long range sound propagation in the deep ocean", *Journal of the Acoustical Society of America*, vol. 33, pp. 456 - 464.
- Hirsch, P. 1965, "Acoustic field of a pulsed source in the underwater sound channel", *Journal of the Acoustical Society of America*, vol. 38, pp. 1018 - 1030.
- Korn, G. A. & Korn, T. M. 1961, "Mathematical handbook for scientists and engineers", McGraw-Hill Book Company, New York.
- McDonald, B. E., Collins, M. D., Kuperman, W. A., & Heaney, K. D. 1994, "Comparison of data and model predictions for Heard Island acoustic transmissions", *Journal of the Acoustical Society of America*, vol. 96, pp. 2357 - 2370.
- Mackenzie, K. V. 1981, "Nine-term equation for sound speed in the oceans", *Journal of the Acoustical Society of America*, vol. 70, pp. 807 - 812.
- National Geophysical Data Center n.d. Retrieved: April 2005, from [http://www.ngdc.noaa.gov/mgg/gdas/gd\\_designagrid.html](http://www.ngdc.noaa.gov/mgg/gdas/gd_designagrid.html)
- Pedersen, M. A. & White, D. 1970, "Ray Theory for Sources and Receivers on an Axis of Minimum Velocity", *Journal of the Acoustical Society of America*, vol. 48, pp. 1219-1248.
- Watson, A. G. D. 1958, "The effect of the earth's sphericity in the propagation of sound in the sea", Report no. N29, Admiralty Research Laboratory, Teddington, England.
- Westwood, E. K., Tindle, C. T., & Chapman, N. R. 1996, "A normal mode model for acousto-elastic ocean environments", *Journal of the Acoustical Society of America*, vol. 100, pp. 3631-3645.
- Williams, A. O. & Horne, W. 1967, "Axial focusing of sound in the SOFAR channel", *Journal of the Acoustical Society of America*, vol. 41, pp. 189 - 198.
- "World Ocean Atlas 1998 (Online Data)" 1998. Retrieved July 2004, from [http://www.nodc.noaa.gov/OC5/data\\_woa.html](http://www.nodc.noaa.gov/OC5/data_woa.html)
- Zhang, Z. Y. 1998, "A semi-empirical expression for source levels of shallow explosive charges", *Proceedings UDT Pacific 98*, pp 459 - 463. Nexus Information Technology, Kent, England.